ORGANOMETALLICS

Article

pubs.acs.org/Organometallics

Exploration of the Mechanism of Platinum(II)-Catalyzed C−F Activation: Characterization and Reactivity of Platinum(IV) Fluoroaryl Complexes Relevant to Catalysis

Tongen Wang, Lauren Keyes, Brian O. Patrick, and Jennifer A. Love*

Department of Chemistry, 2036 Main Mall, University of British Columbia, Vancouver, British Columbia, V6T 1Z1

Supporting Information

ABSTRACT: A series of Pt(IV) complexes relevant to catalytic C−F activation have been prepared and structurally characterized. Pt^{IV}−F complexes, formed by C−F activation, underwent transmetalation with Me_2Zn to generate Me_3Pt^{IV} fluoroaryl complexes. In all cases, the Me_3Pt^{IV} complex underwent reductive elimination to generate methylated organic products. The reactivity of both Pt^{IV}−F and Me_3Pt^{IV} fluoroaryl complexes was strongly affected by the electronic nature of the cyclometalated fluoroaryl ligand.

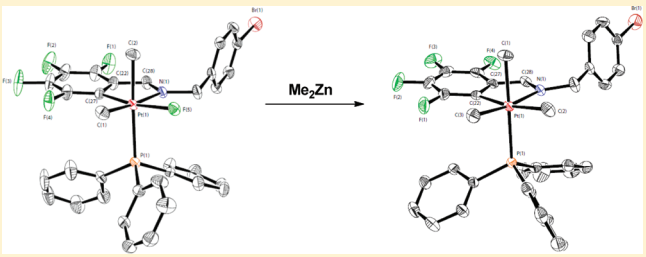

INTRODUCTION

Transition-metal-catalyzed carbon−element bond activation has been an area of much interest in the synthetic community for decades. In particular, late-transition-metal complexes have been extensively utilized as catalysts in cross-coupling reactions, allowing for the construction of C−C and C−X bonds with broad scope.[1] These methodologies permit the assembly of a vast array of molecular frameworks and, as such, are routinely utilized in the preparation of natural products, pharmaceuticals, and materials.

The oxidative addition of a carbon−halogen (C−X) bond across a low-valent metal center is the initial step in many cross-coupling reactions.[2] As a result, transition-metal-mediated C−X bond activation, including C−F bonds, has been well studied.[3] Despite this, examples of catalytic conversion of C−F bonds into C−C bonds are rare in comparison to cross-coupling reactions of other C−X reagents.[4] Therefore, catalytic activation of C−F bonds remains a considerable challenge to the field of organometallic chemistry. Furthermore, the catalytic functionalization of polyfluoroarenes as a means to generate functionalized aryl fluorides is of particular interest, given the increasing prevalence of these moieties in pharmaceuticals,[5] materials,[6] and agrochemicals.[5]

To this end, several groups have developed methods for the activation of fluoroaromatics, with a particular emphasis on using group 9[7] and 10[8] metal complexes. Early transition metals have also been utilized in C−F activation, but to a lesser extent.[9] The first example of a catalytic aryl fluoride cross-coupling was reported by Kumada in 1973.[10a] The process involved the coupling of fluorobenzene with alkyl Grignard reagents, catalyzed by a Ni salt. However, the development of additional methodologies for the catalytic cross-coupling of aryl fluorides is relatively new, with only two additional examples appearing before the turn of the millennium.[10b,c] Building on these initial reports, the application of Stille- and Suzuki-type conditions to the cross-coupling of electron-deficient fluoroarenes has been demonstrated.[10d−i] While important from the standpoint of much-needed defluorination technology, the inability to stop at partial defluorination renders this approach unsuitable for generating functionalized polyfluoroarenes. Methodologies for the selective cross-coupling of polyfluoroarenes are of particular interest, as the products of these reactions (partially functionalized aryl fluorides) have potential for further use as synthetic building blocks. Recently, several reports of catalytic cross-coupling of polyfluoroarenes based on group 9 and 10 metal complexes have emerged.[10j−o]

Our group has developed a methodology for the catalytic methylation of a variety of polyfluoroaryl imines in high yields and high selectivity utilizing a platinum dimer—$[(CH_3)_2Pt(\mu\text{-}SMe_2)]_2$ (eq 1).[11,12] This approach relies on C−F bond

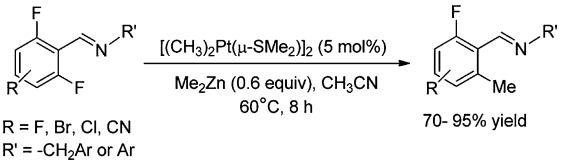

(1)

activation with subsequent functionalization at carbon and is selective for monomethylation. In addition, a range of substitution patterns on the fluoroaryl ring are well-tolerated, as are potentially reactive functional groups.

Mechanistic analysis of Pt(II)-catalyzed methylation is consistent with a typical cross-coupling mechanism—imine-directed C−F activation, transmetalation, and reductive elimination (Scheme 1; geometries not known).[13] The imine

Special Issue: Fluorine in Organometallic Chemistry

Received: August 12, 2011
Published: January 5, 2012

 © 2012 American Chemical Society

Scheme 1. Mechanism of Pt(II)-Catalyzed Methylation of Polyfluoroaryl Imines

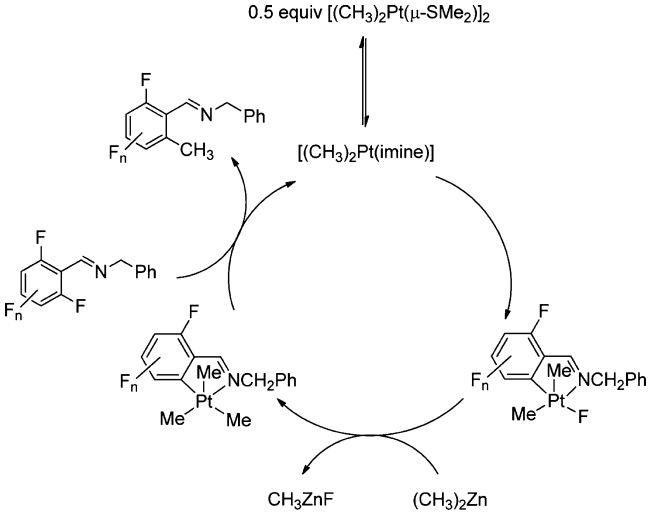

functionality directs C−F activation to the ortho position of the aromatic ring, which accounts for the selectivity of the reaction. This results in the formation of a Pt^{IV}−F complex from which transmetalation with a suitable organometallic reagent and subsequent reductive elimination generates the ortho-functionalized polyfluoroaryl imine products. Each step of the reaction (oxidative addition, transmetalation, and reductive elimination) was impeded by excess SMe_2, as was the catalytic reaction itself. This is consistent with the mechanistic scheme shown, where five-coordinate intermediates are part of the catalytic cycle (vide infra).

A variety of Pt(II) complexes have been found capable of activating strong carbon−element bonds.[14] Indeed, Pt(II)−Pt(IV) systems have been utilized in other catalytic transformations, such as C−H activation.[14] However, in comparison to other group 10 metals, much less is known about the fundamental reactivity of Pt-based catalytic systems, particularly high-valent Pt(IV) complexes. This information is essential to addressing the current limitations of catalytic C−F activation and to expand the reaction scope. Therefore, we were interested in evaluating the reactivity of the Pt(IV) complexes involved in catalytic C−F activation. We disclose herein the characterization and systematic study of the formation and reactivity of a series of Pt(IV) complexes relevant to catalytic C−F activation. These results build upon our proposed mechanism of catalytic methylation and provide deeper insight into each of the fundamental steps involved in catalysis.

■ RESULTS AND DISCUSSION

C−F Activation. We began our studies by investigating the C−F activation of a series of polyfluoroarenes. We had previously found that coordinatively unsaturated Pt^{IV}−F complexes were involved in the catalytic methylation of polyfluoroaryl imines (Scheme 1).[13] In addition, it was determined that Pt^{IV}−F·SMe_2 complexes, which would be formed by SMe_2 recoordination, could re-enter the catalytic cycle.[13] Importantly, these Me_2Pt^{IV}−F complexes did not undergo reductive elimination to give either methylated imine products or ethane. Given the important role of Pt^{IV}−F complexes in catalysis, we sought to gain more information about the structure and reactivity of these complexes.

Pt^{IV}−X·SMe_2 (X = F, Br) complexes were easily prepared by treating a given polyfluoroaryl imine with a stoichiometric amount of $[(CH_3)_2Pt(\mu\text{-}SMe_2)]_2$. We were interested in evaluating electronic effects on the overall reactivity of these Pt^{IV}−X complexes. To this end, Pt^{IV}−X complexes with fully fluorinated (**1**) and partially fluorinated (**2**[16a] and **3**) cyclometalated ligands were prepared (Scheme 2). The Pt^{IV}−Br

Scheme 2. Preparation of Pt^{IV}−X (X = Br, F) Complexes

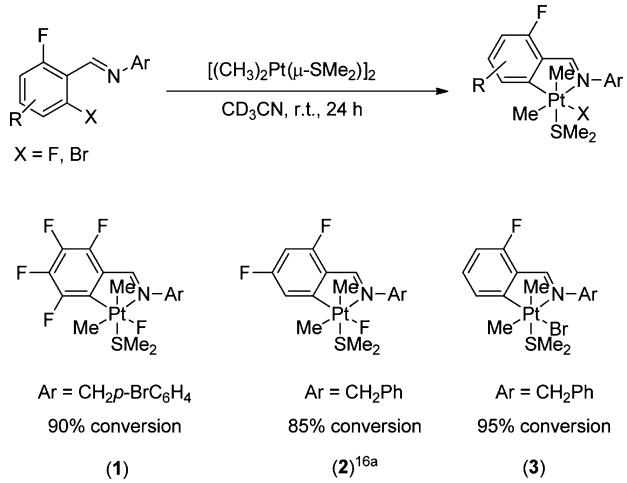

complex **3** was prepared using *N*-(2-bromo-6-fluorobenzylidene)benzylamine; the corresponding Pt^{IV}−F complex could not be prepared because of the low reactivity of *N*-(2-fluoro-6-fluorobenzylidene)benzylamine (vide infra).

The lability of the SMe_2 ligand has largely impeded the isolation and solid-state characterization of the Pt^{IV}−X·SMe_2 complexes. Nevertheless, the geometry of these complexes could be determined on the basis of *in situ* solution state NMR spectroscopy. The chemical shift and coupling constant data for complex **2** match the published data[15,16a] and are given in Table 1 for comparison with complexes **1** and **3**. As expected on the basis of the work of Crespo and Martinez on **2** and other related complexes,[16a] diagnostic features in the ^1H and ^{19}F NMR spectra are indicative of the formation of Pt^{IV}−F bonds in the new complexes **1** and **3**. For each complex, the ^{19}F NMR spectrum shows a broad signal corresponding to the Pt−F bond; the signal (δ −250 to −270) is considerably upfield relative to other aryl F signals. Characteristic ^1H NMR spectral data for **1**−**3** are summarized in Table 1.[17] Imine coordination to Pt is evident in the ^1H NMR spectra by the presence of a singlet, with Pt satellites, ranging from δ 8.88 to 8.23 (Table 1, entry 1). In addition, the presence of two upfield signals (δ 1.50−0.80, with coupling to both Pt and F) are consistent with the formation of new Pt−Me bonds (Table 1, entries 3 and 4). The F−H coupling constants are consistent with a cis orientation of fluorine to both methyl ligands. The Pt−H coupling constants indicate that the methyl groups are trans to L-type donor ligands.[18] This indicates that the fluorine ligand is trans to the cyclometalated fluoroaryl ligand (as depicted in Table 1). The same geometry was also observed with a related Pt^{IV}−Br complex (**3**). NOE data confirmed the geometrical assignments for all complexes.[18]

Previous studies established that the labile SMe_2 ligand could be substituted with PPh_3.[16] On this basis, we sought to convert **1**−**3** to the corresponding Pt^{IV}−F·PPh_3 complexes. Displacement of SMe_2 with PPh_3 occurred readily at room temperature

Table 1. Characteristic ^{1}H NMR Spectroscopic Data for Complexes 1, 2,[a] and 3

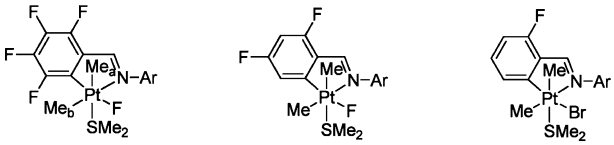

Ar = CH_2*p*-BrC_6H_4 (1) | Ar = CH_2Ph (2)[a] | Ar = CH_2Ph (3)

entry	assignt	δ (multiplicity)[b]	δ (multiplicity)[a,b]	δ (multiplicity)[b]	rel intens
1	CH═N	8.98 (s, J_{Pt-H} = 48.0 Hz)	8.23 (s, J_{Pt-H} = 55.2 Hz)	8.40 (s, J_{Pt-H} = 48.7 Hz)	1
2	Pt−SMe_2	1.96 (s, J_{Pt-H} = 12.0 Hz)	1.89 (s, J_{Pt-H} = 12.0 Hz)	1.87 (s, J_{Pt-H} = 12.0 Hz)	6
3	Pt−Me_b	1.50 (dd, J_{Pt-H} = 63.0 Hz, J_{F-H} = 6 Hz)	1.11 (d, J_{Pt-H} = 65.7 Hz, J_{F-H} = 8 Hz)	1.07 (s, J_{Pt-H} = 68.4 Hz)	3
4	Pt−Me_a	0.80 (d, J_{Pt-H} = 66.0 Hz, J_{Pt-F} = 6 Hz)	0.72 (d, J_{Pt-H} = 68.1 Hz, J_{Pt-F} = 8 Hz)	0.71 (s, J_{Pt-H} = 69.6 Hz)	3

[a]NMR spectral data are consistent with previously reported characterization data for this compound.[16a] [b]NMR spectral data were obtained under the following conditions: acetonitrile-d_3, 25 °C, 300 MHz.

(Scheme 3). The reactions were monitored by ^{1}H, ^{19}F, and ^{31}P{^{1}H} NMR spectroscopy. Our data for complex **5**[16a] match the published data and are given in Table 2 for comparison with complexes **4** and **6**.

Scheme 3. Preparation of Pt^{IV}−X·PPh_3 (X = F, Br) Complexes

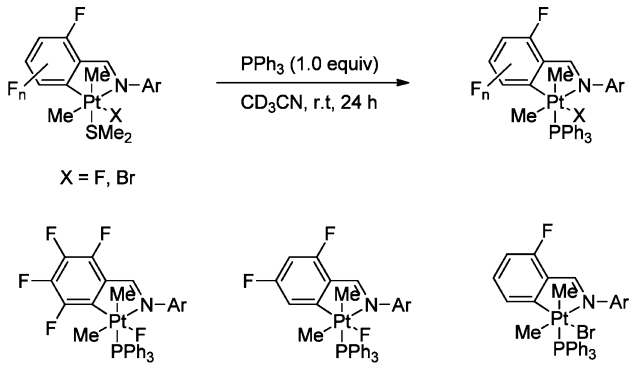

Complexes **4** and **6** were characterized by multinuclear NMR spectroscopy, NOE, HRMS, and X-ray diffraction[18] The formation of the corresponding Pt^{IV}−F·PPh_3 complexes is clearly indicated by the ^{1}H and ^{31}P{^{1}H} NMR spectra (Table 2). The presence of large satellite signals in the ^{31}P{^{1}H} NMR spectra, corresponding to Pt−P coupling (Table 2; entry 4), are consistent with PPh_3 coordination. The chemical shift of the PPh_3 signal is within the range reported for related Pt−PPh_3 complexes.[16] In the ^{1}H NMR spectra, coordination of PPh_3 can be seen indirectly through the additional splitting of the Pt−Me resonances. This new splitting is the result of coupling between multiple NMR-active nuclei, giving rise to F−H, P−H, and Pt−H coupling constants as well as complex multiplets (Table 2; entries 2 and 3).

In addition to changes in multiplet structure, coordination of PPh_3 was also found to shift various resonances in the ^{1}H NMR spectra relative to the SMe_2 complexes. The most significant effect was observed for the CH═N resonances of the various Pt(IV) complexes. For example, the CH═N resonance for the Pt^{IV}−F·PPh_3 complex **4** shifted upfield by δ 0.42 in comparison to that for the Pt^{IV}−F·SMe_2 complex **1** (compare Table 1, entry 1, and Table 2, entry 1). This is consistent with the stronger σ-donating ability of the PPh_3 ligand relative to that of SMe_2, resulting in a more electron rich Pt center. In general, the apical

Table 2. NMR Spectroscopic Data for Complexes 4, 5,[a] and 6

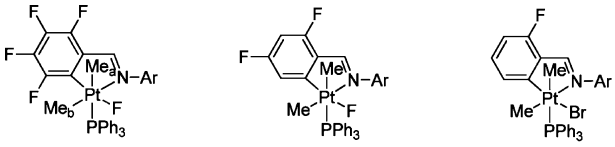

Ar = CH_2*p*-BrC_6H_4 (4) | Ar = CH_2Ph (5)[a] | Ar = CH_2Ph (6)

entry	assignt	δ (multiplicity)[c]	δ (multiplicity)[a,b]	δ (multiplicity)[c]	rel intens
1	CH═N	8.56 (s, J_{Pt-H} = 36.9 Hz)	8.23 (s, J_{Pt-H} = 55.2 Hz)	8.11 (s, J_{Pt-H} = 49.8 Hz)	1
2	Pt−Me_b	1.62 (m, J_{Pt-H} = 59.4 Hz, J_{F-H} = 12 Hz, J_{P-H} = 5 Hz)	1.22 (td, J_{Pt-H} = 66.0 Hz, J_{P-H} = 8 Hz) (J_{F-H} = 2 Hz)	1.49 (d, J_{Pt-H} = 69.3 Hz, J_{P-H} = 8 Hz)	3
3	Pt−Me_a	0.74 (td, J_{Pt-H} = 61.0 Hz, J_{P-H} = 12 Hz, J_{F-H} = 5 Hz)	0.62 (td, J_{Pt-H} = 61.8 Hz, J_{P-H} = 8 Hz, J_{F-H} = 2 Hz)	0.98 (d, J_{Pt-H} = 58.2 Hz, J_{P-H} = 8 Hz)	3
4	Pt−PPh_3	−0.57 (d, J_{Pt-P} = 1614 Hz, J_{F-P} = 52 Hz)	−1.72 (d, J_{Pt-P} = 1102 Hz, J_{F-P} = 64 Hz)	−7.2 (d, J_{Pt-P} = 1005 Hz)	N/A

[a]NMR spectral data are consistent with the previously reported characterization data for this compound.[16a] [b]NMR spectral data were obtained under the following conditions: acetonitrile-d_3, 25 °C, 300 MHz. [c]NMR spectral data were obtained under the following conditions: dichloromethane-d_2, 25 °C, 300 MHz.

methyl ligand was more affected by PPh_3 coordination, as observed by greater changes in chemical shift (compare Tables 1 and 2, entry 3). Such a result is expected on the basis of the trans influence of ligands in octahedral complexes.[2] As with our characterization of the related Pt^{IV}–F·SMe_2 complexes, the geometry of these Pt^{IV}–F·PPh_3 complexes was confirmed by NOE analysis.[18]

Single crystals of complexes **4** and **6** were obtained from saturated solutions of acetonitrile (Figure 1). Selected bond lengths and bond angles are summarized in Table 3. Crystallographic parameters are given in Table 4. The solid-state molecular structures of complexes **4** and **6** clearly demonstrate the octahedral geometry of the platinum metal center (Figure 1). The square plane is defined by C1, C27/C22, N1, and X (X = F, Br), with C2 and P1 occupying the apical positions. Examination of the bonding data for complexes **4** and **6** reveals many structural similarities between the two Pt^{IV}–F complexes. Specifically, the Pt–C_{aryl} and Pt–N bond lengths for both complexes are equivalent, within experimental error (entries 4 and 6, Table 3). The Pt–C bond lengths for both complexes, which range from 2.04 to 2.09 Å, are within the range reported for other similar Me_2Pt^{IV}–X complexes.[16] For all complexes, the Pt–C2 bond, which corresponds to the methyl group trans to PPh_3, is longer than the Pt–C1 bond, which corresponds to the methyl group trans to the nitrogen of the imine (Table 3, entry 2). The increased bond length is consistent with the smaller Pt–H coupling observed for this methyl ligand in all complexes (Table 3, entry 2).

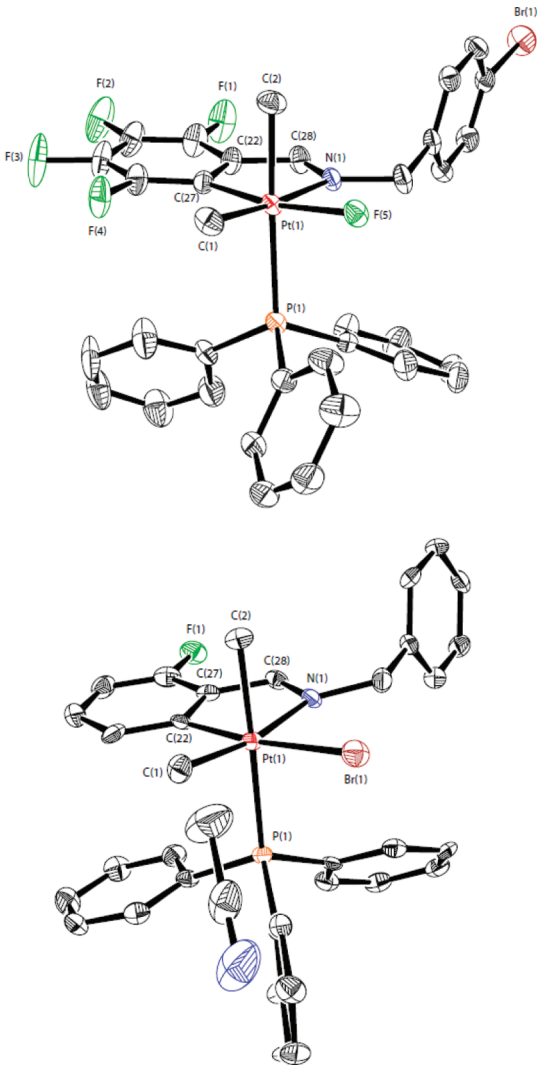

Figure 1. ORTEP representation of the solid-state molecular structures of complexes **4** (top) and **6** (bottom) (ellipsoids plotted at 50% probability, hydrogen atoms removed for clarity).

Table 3. Selected Bond Lengths (Å) and Angles (deg) for Complexes 4 and 6

	4		6	
entry				
1	Pt1–F5	2.0469(17)	Pt1–Br	2.5657(8)
2	Pt1–C1	2.065(3)	Pt1–C1	2.049(7)
3	Pt1–C2	2.075(3)	Pt1–C2	2.093(7)
4	Pt1–N1	2.139(3)	Pt1–N1	2.144(6)
5	Pt1–P2	2.4259(8)	Pt1–P1	2.4146(17)
6	Pt1–C27	1.997(3)	Pt1–C22	2.004(7)
7	N1–C36	1.276(4)	N1–C28	1.288(9)
8	C1–Pt1–F5	88.49(11)	C1–Pt1–Br1	91.4(2)
9	C1–Pt1–C27	99.56(14)	C1–Pt1–C22	93.0(3)
10	F5–Pt1–N1	91.01(9)	Br1–Pt1–N1	94.51(16)
11	C27–Pt1–N1	80.28(11)	C22–Pt1–N1	80.5(2)
12	C1–Pt1–C2	87.47(15)	C1–Pt1–C2	86.4(3)
13	C2–Pt1–F5	86.38(12)	C2–Pt1–Br1	88.2(2)
14	C27–Pt1–F5	169.06(11)	C22–Pt1–Br1	173.47(18)
15	C1–Pt1–P1	90.84(10)	C1–Pt1–Br1	92.71(2)
16	F5–Pt–P1	89.79(6)	Br1–Pt1–P1	93.47(5)

Table 4. Crystallographic Data for Complexes 4 and 6

	4	6
empirical formula	$C_{36}H_{35}N_2FPPtBr$	$C_{34}H_{28}NPPtF_5Br$
formula wt	820.63	851.54
cryst syst	monoclinic	monoclinic
space group (No.)	$P2_1/n$ (14)	$C2/c$ (15)
a (Å)	9.4945(7)	28.4705(10)
b (Å)	18.1068(11)	9.0217(3)
c (Å)	18.3770(10)	27.1319(14)
α (deg)	90.0	90.0
β (deg)	90.972(3)	118.750(1)
γ (deg)	90.0	90.0
V (A^3)	3158.8(3)	6109.8(4)
Z	4	8
D_c (g/cm^3)	1.726	1.851
T (K)	173 ± 1	173 ± 1
solvent/color	acetonitrile/ colorless	acetonitrile/ colorless
F(000)	1608.00	3296.00
$2\theta_{max}$ (deg)	50.8	55.8
total no. of rflns collected	16 842	40 367
no. of unique rflns ($F > 4\sigma(F)$)	5795	7250
R_{int}	0.039	0.037
R1, wR2 ($I > 2\sigma(I)$)	0.038, 0.091	0.025, 0.054
GoF	1.1	1.04
peak, hole (e/Å^3)	2.10, −0.88	1.06, −1.00

Transmetalation. Following C–F activation, the next step in our proposed mechanism involves transmetalation between dimethyl zinc and a Pt^{IV}–F species to generate a $Me_3Pt(IV)$ complex (Scheme 1). We had previously determined that a Me_3Pt^{IV} complex was formed during the course of catalytic methylation of *N*-(2,4,6-trifluorobenzylidene)benzylamine (**7**).[13] Several small signals, corresponding to Pt–Me resonances,

were observed in the ^{1}H and ^{19}F NMR spectra in low concentration throughout the course of the reaction and were eventually depleted. Comparison of these spectra with that of independently synthesized Me_3Pt^{IV} complex **8** confirmed this assessment; although we were unable to isolate complex **8**, we were able to obtain NMR spectral data of the crude product.[13] The addition of a solution of complex **8** to a catalytic sample resulted in an increase in those signals which we had attributed to formation of a Me_3Pt^{IV} complex during the course of catalytic methylation. On this basis, we postulated the mechanism to involve initial formation of a Pt^{IV}−F complex via imine C−F activation followed by transmetalation with dimethylzinc to generate a Me_3Pt^{IV} complex that is the catalyst resting state (Scheme 4).[13]

Scheme 4. Methylation of *N*-(2,4,6-Trifluorobenzylidene)benzylamine (7)

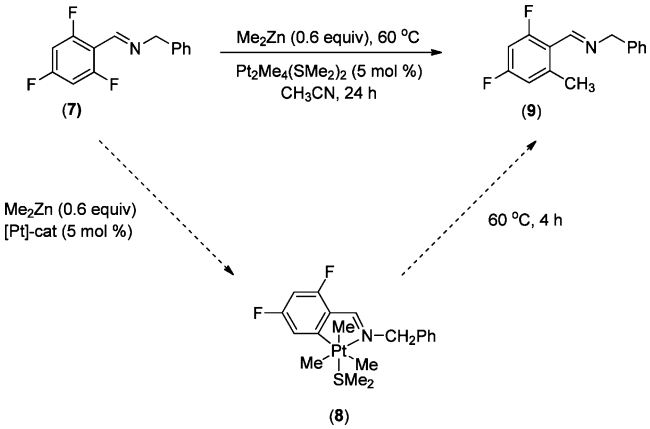

In order to obtain more complete characterization data for Me_3Pt^{IV} complexes resulting from transmetalation, we sought to prepare and isolate complexes of this type. We anticipated that the SMe_2 complexes were too reactive for isolation but that the corresponding PPh_3 complexes should be isolable. We now report the synthesis and characterization of $Me_3Pt^{IV}{\cdot}PPh_3$ complex **11**, which contains a perfluorinated cyclometalated ligand.[21]

Complex **11** was readily prepared by treatment of the Me_2Pt^{IV}−F·PPh_3 complex **10** with dimethylzinc (eq 2).

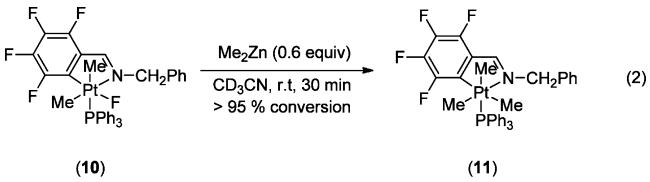

(2)

Alternatively, complex **11** could be prepared by treatment of the corresponding Me_2Pt^{IV}−F·SMe_2 complex with dimethyl zinc followed by ligand exchange with PPh_3.[18] Both processes proceeded in high conversion.

This complex was characterized by multinuclear NMR spectroscopy and X-ray diffraction, and diagnostic signals for $Me_3Pt^{IV}{\cdot}PPh_3$ complex **11** are included in Table 5. The presence of an imine signal with Pt satellites as well as three upfield Pt−Me signals of equal intensity are general features of Me_3Pt^{IV} complexes. Importantly, each of the Pt−Me signals can be attributed to a specific methyl ligand on the basis of the ^{1}H NMR data.[18] More specifically, the multiplet at δ 1.38 (dd, J_{Pt-H} = 70.5 Hz, J_{P-H} = 8 Hz, J_{F-H} = 2 Hz) can be assigned as Me_b, the methyl group in the plane of the fluoroaryl ring, on the basis of the additional F−H coupling (entry 3). The smaller Pt−H coupling associated with the signal at δ 0.66 (d, J_{Pt-H} = 48.0 Hz, J_{P-H} = 8 Hz) is consistent with a methyl group that is trans to an X-type ligand (the fluoroaryl ring) (entry 4). Finally, the signal at δ 0.46 (d, J_{Pt-H} = 63.8 Hz, J_{P-H} = 8 Hz) has large Pt−H coupling, which we previously determined was the result of a trans orientation relative to an L-type (PPh_3) ligand (entry 5).

Crystals of $Me_3Pt^{IV}{\cdot}PPh_3$ complex **11** were obtained by layering pentanes on a saturated solution of dichloromethane. The solid-state molecular structure is depicted in Figure 2, with selected bond lengths and bond angles given in Table 6. Crystallographic parameters are summarized in Table 7.

The solid-state molecular structure of complex **11** clearly illustrates that there are three methyl ligands attached to the Pt center. In addition, complex **11** has an octahedral geometry in which the square plane is defined by the cyclometalated fluoroaryl ring as well as C2/C3 atoms. The C1 methyl and PPh_3 ligands adopt the apical positions in both structures. This same geometry was observed for complexes **4** and **6** as well as in related structures reported by Crespo and Martinez.[16] Interestingly, in all complexes, the Pt−C2 bonds are the longest, in comparison to the other Pt−Me bond lengths (Table 6, entries 1 −3). This is consistent with the expected formation of a particularly strong C_{aryl}−Pt bond due to the highly electron deficient cyclometalated fluoroaryl ring.[21] However, the remaining bond lengths and bond angles for these complexes are essentially identical, within experimental error, with those calculated for Me_2Pt^{IV}−F·PPh_3 complexes **4** and **6** (Table 6).

We next sought to examine the role of ligand dissociation in transmetalation by comparing the relative rates of transmetalation of Pt^{IV}−F·SMe_2 complex **2** in the presence and absence of excess SMe_2 (eqs 3 and 4). Although transmetalation

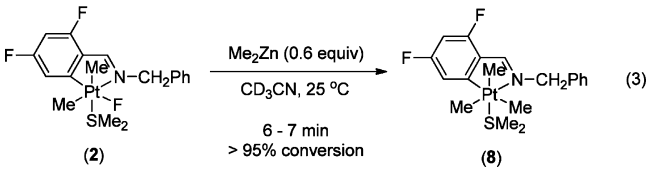

(3)

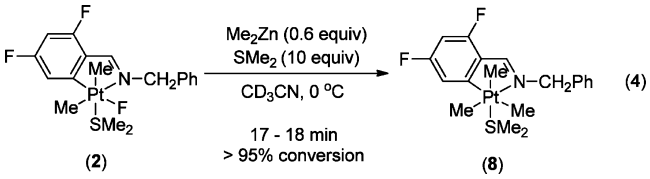

(4)

proceeded too rapidly at room temperature for analysis, we were able to monitor the reaction at 0 °C using VT NMR spectroscopy.[18] The rate of transmetalation was slowed by the presence of excess SMe_2, which is consistent with a mechanism that proceeds via a pentacoordinate complex.

Additional evidence for rapid dissociation and reassociation of SMe_2 was obtained through an isotopic labeling experiment. A deuterium-labeled Pt(II) complex, $Pt_2(CD_3)_2(SMe_2)_2$, was used to generate $(CD_3)_2Pt^{IV}$−F·SMe_2 complex **13**. Subsequent transmetalation with Me_2Zn resulted in complete scrambling of

Table 5. ^{1}H NMR Chemical Shifts for Complex 11[a]

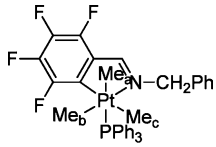

(11)

entry	δ	multiplicity	rel intens	assignt
1	8.48	s (J_{Pt-H} = 41.1 Hz)	1	CH═N
2	4.39	dd (J_{H-H} = 15.6 Hz) AB pattern	2	CH_2
3	1.38	dd (J_{Pt-H} = 70.5 Hz, J_{Pt-H} = 8 Hz, J_{Pt-H} = 2 Hz)	3	Me_b–Pt
4	0.66	d (J_{Pt-H} = 63.8 Hz, J_{P-H} = 8 Hz)	3	Me_c–Pt
5	0.46	d (J_{Pt-H} = 63.8 Hz, J_{P-H} = 8 Hz)	3	Me_a–Pt

[a]NMR spectral data were obtained under the following conditions: acetonitrile-d_3, 25 °C, 300 MHz.

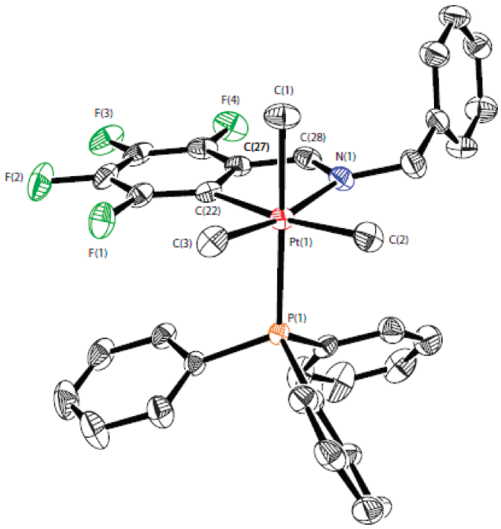

Figure 2. ORTEP representation of the solid-state molecular structure of complex **11** (ellipsoids plotted at 50% probability, hydrogen atoms removed for clarity).

Table 6. Selected Bond Lengths (Å) and Angles (deg) for Complex 11

entry		
1	Pt1–C1	2.076(2)
2	Pt1–C2	2.095(2)
3	Pt1–C3	2.057(2)
4	Pt1–N1	2.1435(17)
5	Pt1–P1	2.3743(5)
6	Pt1–C22	2.099(2)
7	N1–C28	1.280(3)
8	C3–Pt1–C2	89.43(10)
9	C3–Pt1–C22	97.49(9)
10	C2–Pt1–N1	93.33(8)
11	C22–Pt1–N1	78.81(8)
12	C3–Pt1–C1	87.37(9)
13	C1–Pt1–C2	86.52(10)
14	C22–Pt1–C2	169.52(8)
15	C2–Pt1–P1	92.64(7)
16	C3–Pt1–P1	90.67(7)

the deuterium labeling at room temperature, as indicated by the 1:1:1 ratio of the Pt–Me signals in the ^{1}H NMR spectrum (eq 5). This result is consistent with transmetalation being dissociative in SMe_2 and also indicates that isomerization of the resulting pentacoordinate species is similar to that in other $(CH_3)_nPt^{IV}$ complexes.[22]

Table 7. Crystallographic Data for Complex 11

empirical formula	$C_{35}H_{31}NF_4PPtBr$
formula wt	847.58
cryst syst	triclinic
space group (No.)	$P\bar{1}$ (2)
a (Å)	10.5281(7)
b (Å)	10.5282(7)
c (Å)	15.3290(15)
α (deg)	86.304(3)
β (deg)	76.090(3)
γ (deg)	69.947(3)
V (Å^3)	1548.98(18)
Z	2
D_c (g/cm^3)	1.817
T (K)	173
solvent/color	pentanes/pink
F(000)	824.00
$2\theta_{max}$ (deg)	56.2
total no. of rflns collected	33 132
no. of unique rflns ($F > 4\sigma(F)$)	7494
R_{int}	0.036
R1, wR2 ($I > 2\sigma(I)$)	0.020, 0.041
GOF	1.04
peak, hole (e/A^3)	0.74, −0.88

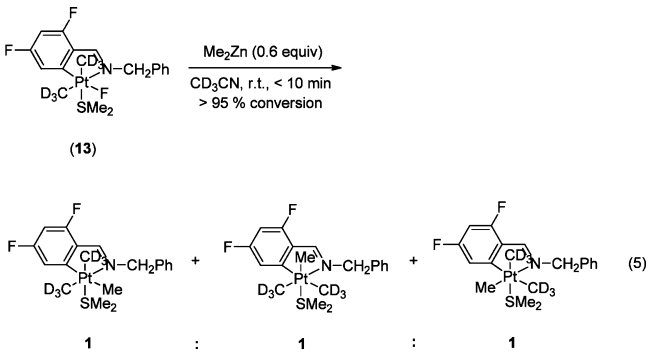

Reductive Elimination. During the course of our initial investigations of Pt(II)-catalyzed C–F activation, we discovered that Me_3Pt^{IV} complexes, upon heating, underwent reductive elimination to generate the corresponding methylated imines in high conversion (eq 6).[13,23]

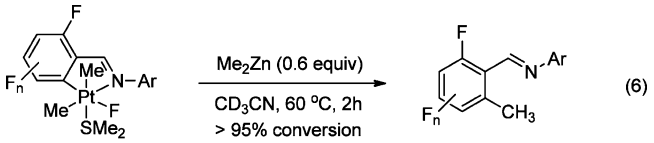

Ar =CH_2Ph, Ph

Interestingly, we observed a correlation between the rate of reductive elimination and the number of fluorine substituents on the cyclometalated fluoroaryl ring. The reaction half-lives for reductive elimination of several Me_3Pt^{IV} complexes are summarized in Scheme 5. The slowest rate of reductive elimination was observed for the Me_3Pt^{IV} complex derived from **14**, whereas Me_3Pt^{IV} complexes **8** and **15** underwent reductive elimination at a greater rate (Scheme 5). Electron-withdrawing ligands are known to reduce the rate of reductive elimination.[21] The implications of these results on the catalytic methylation of polyfluoroaryl imines is discussed in greater detail in the following section (vide infra).

Scheme 5. Reductive Elimination of Me_3Pt^{IV} Complexes

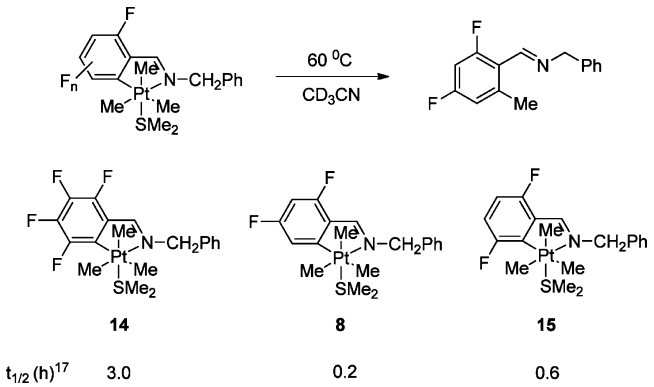

Given the involvement of coordinatively unsaturated Pt(IV) complexes in both C−F activation and transmetalation, we sought to examine whether reductive elimination also proceeds via a dissociative mechanism. The addition of excess SMe_2 (10 equiv) to a mixture of Me_3Pt^{IV} complex **8** resulted in <20% product formation after 1 h at 60 °C (eq 7). Under standard conditions, reductive elimination from complex **8** proceeds to give the methylated imine **9** in 69% yield over the same time interval (eq 8). The net effect of excess SMe_2 on the rate of reductive elimination is consistent with a dissociative mechanism.

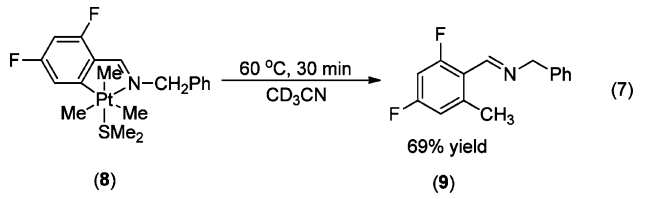

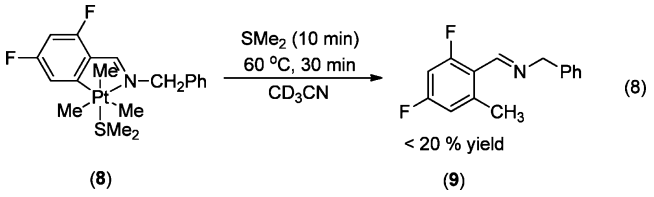

Comparison between Stoichiometric Studies and Catalytic C−F Activation. We had previously reported comparable trends for stoichiometric C−F activation and catalytic cross-coupling, which was consistent with C−F activation being part of the catalytic cross-coupling mechanism.[13] We anticipated that the rate-determining step may change, depending on the degree of fluorination. This prompted us to compare the rates of C−F activation, reductive elimination, and catalytic methylation for a few fluoroaryl imines. Table 8 summarizes the half-lives for C−F activation and the yields of catalytic methylation. The half-lives for reductive elimination were previously given in Scheme 5.

As was the case with reductive elimination, both stoichiometric C−F activation and catalytic methylation were significantly influenced by the degree of fluorination of the polyfluoroaryl imine. Crespo and Martinez reported that the rates of C−F activation were fastest for the most heavily fluorinated imines, consistent with their proposed oxidative addition mechanism.[16a] Our results confirmed these observations (Table 8, column 1).[13] A comparison of some catalytic reactions provides additional insight. Whereas imines **7** and **17** were readily converted to their corresponding methylated products in 8 h at 60 °C, the reaction of perfluorinated imine **16** required heating to 80 °C for 12 h (Table 8, column 2). The reaction was simply slow; the low rate was not due to decomposition or byproduct formation.[13] These results can be rationalized by considering the differences in the stability of the intermediate Pt(IV) complexes. The ability of electron-deficient ligands to stabilize high-valent metal complexes has been extensively documented.[21] This effect has been attributed to the increased strength of the resulting M−C bonds in complexes containing electron-deficient ligands. Therefore, the high reactivity of complex **14** (derived from imine **16**) toward stoichiometric C−F activation can be attributed to the favorable formation of a more stable Pt(IV) complex. Similarly, the lower catalytic turnover of imine **16** compared with those of **7** and **17** is a direct result of this increased stability. This is consistent with the observed slower reductive elimination from **14** (Scheme 5).

These results are indicative of a change in the rate-determining step depending on the degree of fluorination For substrates with a lesser degree of fluorination (e.g., **7** and **17**), C−F activation is rate-limiting. For substrates with a greater degree of fluorination (e.g., **16**), reductive elimination is rate-limiting. As a result, these findings have a significant impact on the choice of catalytic reaction conditions.

It is also noteworthy to compare imines **7** and **17** (Scheme 6). These substrates were previously found to have comparable catalytic reactivity (Table 8, entries 2 and 3).[11] However, there were subtle differences in the reactivity of these two substrates toward stoichiometric C−F activation as well as reductive elimination. Imine **17** was somewhat more reactive than imine **7** toward stoichiometric C−F activation, yet the resulting Me_3Pt^{IV} complex undergoes reductive elimination more slowly. Both results are consistent with a presumed effect of the *o*-fluorine present in imine **17**.[21] The selectivity for C−F activation in **17** is dictated by the formation of a more stable $Pt^{IV}-C_{aryl}$ bond. The Pt(IV) intermediates derived from **17** are presumably more stable than those derived from **7**, due to the *o*-fluorine in the former. Complex **15** is, thus, more resistant to reductive elimination. However, imines **7** and **17** have similar

Table 8. Comparison of Stoichiometric and Catalytic Reactivity for Polyfluoroaryl Imines

entry	substrate	stoichiometric C-F activation ($t_{1/2}$, h)[a,b]	catalytic methylation[c]	reductive elimination ($t_{1/2}$ h)[f]
1	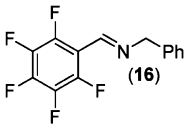 (16)	0.3	74%[d]	3.0
2	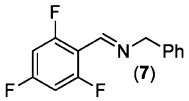 (7)	2.8	95%[e]	0.2
3	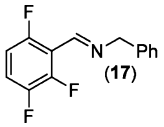 (17)	2.2	92%[e]	0.6

[a]NMR spectral data were acquired under the following conditions: acetonitrile-d_3, 60 °C, 300 MHz. [b]Reaction progress was monitored by ^{1}H and ^{19}F NMR spectroscopy, and results are the average of two independent experiments. Additional details are included in the Supporting Information. [c]Taken from ref 11. [d]Conditions: CH_3CN, Me_2Zn (0.6 equiv), 80 °C, 12 h. [e]Conditions: CH_3CN, Me_2Zn (0.6 equiv), 60 °C, 8 h. [f]Data are the same as those presented in Scheme 5 and are included here for clarity. Details regarding the experimental conditions are included in the Supporting Information.

Scheme 6. Reactivity of Imines 7 and 17

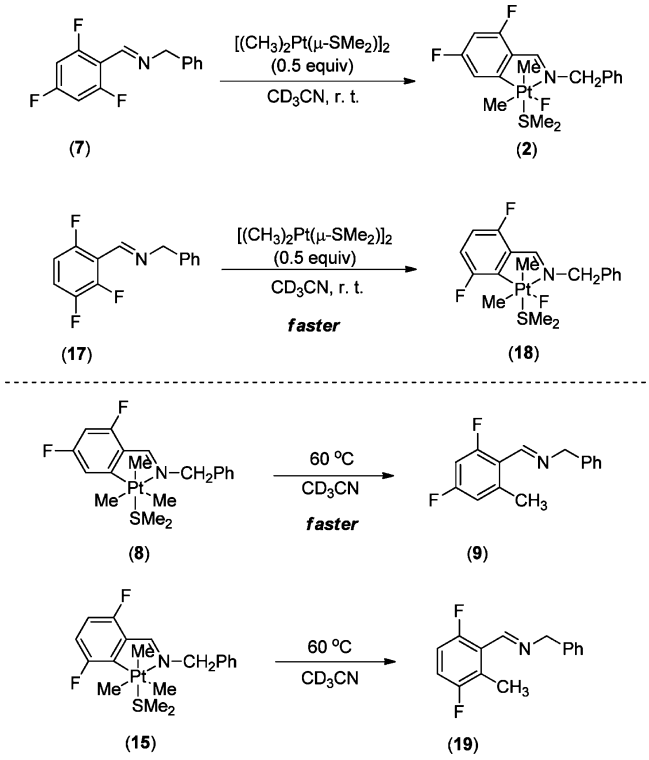

rates and yields of catalytic methylation, because C−F activation is rate-limiting for these substrates.

■ SUMMARY AND CONCLUSIONS

In summary, the synthesis and reactivity of a series of Pt(IV) fluoroaryl complexes have been described. In general, polyfluoroaryl substrates that displayed reasonable catalytic reactivity also underwent stoichiometric C−F activation to form the corresponding Pt^{IV}−F complexes. Subsequent transmetalation with dimethylzinc resulted in formation of the related Me_3Pt^{IV} complexes. While both Pt^{IV}−F·SMe_2 and Me_3Pt^{IV}·SMe_2 complexes proved to be too unstable to isolate, the corresponding PPh_3 complexes were isolable. Heating of Me_3Pt^{IV}·SMe_2 complexes resulted, in all cases, in reductive elimination to generate the same methylated imines that were formed by catalytic methylation. Heavily fluorinated polyfluoroarenes were most effective at directing C−F activation; however, the resulting Me_3Pt^{IV} complexes were resistant toward reductive elimination. These results suggest that while C−F activation is the rate-determining step of catalysis for the majority of the substrates, reductive elimination is rate-limiting for highly activated polyfluoroarenes. Excess SMe_2 impeded each reaction (C−F activation, transmetalation, reductive elimination), consistent with a mechanism in which the catalytically active Pt(IV) species are pentacoordinate. More detailed investigations of reductive elimination from Pt(IV) fluoroaryl complexes is ongoing and will be reported in due course.

■ EXPERIMENTAL SECTION

General Procedures. Manipulation of organometallic compounds was performed using standard Schlenk techniques under an atmosphere of dry nitrogen or in a nitrogen-filled Vacuum Atmospheres drybox (O_2 <2 ppm). NMR spectra were recorded on Bruker Avance 300, Bruker Avance 400, and Bruker Avance 600 spectrometers. ^{1}H and ^{13}C chemical shifts are reported in parts per million and are referenced to residual solvent. Coupling constant values were extracted assuming first-order coupling. The multiplicities are abbreviated as follows: s = singlet, d = doublet, t = triplet, m = multiplet. All spectra were obtained at 25 °C. Mass spectra were recorded on a Kratos MS-50 mass spectrometer. Elemental analyses were performed using a Carlo Erba EA 1108 Elemental Analyzer. Single-crystal X-ray structure determinations were performed by Dr. Brian O. Patrick at the Department of Chemistry, University of British Columbia, using a Bruker X8 Apex CCD area detector with graphite-monochromated Mo Kα radiation.

Material and Methods. Acetonitrile and dichloromethane were dried by heating to reflux over calcium hydride, stored over molecular sieves, and degassed prior to use. Pentanes and hexanes were purified and dried by passage through a column of activated alumina and sparged with dinitrogen prior to use. Acetonitrile-d_3 was obtained from Cambridge Isotopes Inc. and degassed prior to use. All organic

reagents were obtained from commercial sources and used as received. 1,3,5-Trimethoxybenzene was sublimed prior to use. K_2PtCl_4 was purchased from Strem Chemicals and was used without further purification. $PtCl_2(SMe_2)_2$, $Pt_2Me_4(SMe_2)_2$, and $Pt_2(CD_3)_4(SMe_2)_2$ were prepared using previously reported procedures.[24] Dimethylzinc (1.2 M solution in toluene) was purchased from Aldrich and titrated with LiCl and I_2 prior to use.[25]

Preparation of Polyfluoroarenes. All substrates were prepared according to literature procedures. Analytical data match previously reported data.[11] See the Supporting Information for details.

General Procedure for Preparation of Pt^{IV}−F·SMe_2 Complexes. In a 20 mL vial in the glovebox, the polyfluoroarene substrate (0.034 mmol, 1.0 equiv) and $Pt_2Me_4(SMe_2)_2$ (0.017 mmol, 0.5 equiv) were dissolved in dried, degassed CD_3CN (1.0 mL). The resulting solution was transferred to a screw-cap NMR tube containing a septum, which was sealed and removed from the glovebox. The reaction was monitored by ^1H and ^{19}F NMR spectroscopy. Analytical data for all Pt complexes are included in the Supporting Information. Select Pt complexes are included below.

[PtMe$_2$F(SMe$_2$)C$_6$F$_4$CH═NCH$_2$C$_6$H$_4$Br)] ***(1)***. Based on in situ NMR spectroscopic characterization, 90% conversion based on integration of the ^{19}F NMR spectrum. ^1H NMR (acetonitrile-d_3, 300 MHz): δ 8.98 (s, J_{Pt-H} = 48.0 Hz, CH═N, 1H), 7.67−7.45 (m, aryl H, 4H), 5.02 (m, 2H), 1.96 (s, J_{Pt-H} = 12.0 Hz, $S(CH_3)_2$, 6H), 1.50 (dd, J_{Pt-H} = 63.0 Hz, J_{F-H} = 9 Hz, J_{F-H} = 6 Hz, Pt−CH_3, 3H), 0.80 (d, J_{Pt-H} = 66.0 Hz, J_{F-H} = 6 Hz, Pt−CH_3, 3H). ^{19}F NMR (acetonitrile-d_3, 282 MHz): δ −128.2 (m, aryl F, 1F), −139.4 (m, aryl F, 1F), −148.0 (m, aryl F, 1F), −162.8 (m, aryl F, 1F), −253.5 (m, J_{Pt-H} = 175 Hz, Pt−F, 1F).

[PtMe$_2$F(SMe$_2$)(C$_6$F$_2$CH═NCH$_2$C$_6$H$_5$)] ***(2)***. Based on in situ NMR spectroscopic characterization, 85% conversion based on integration of the ^{19}F NMR spectrum. ^1H NMR (acetonitrile-d_3, 300 MHz): δ 8.78 (s, J_{Pt-H} = 47.5 Hz, CH═N, 1H), 7.70−6.60 (m, overlapping peaks, aryl H), 5.05 (m, CH_2, 2H), 1.90 (s, J_{Pt-H} = 12.1 Hz, $S(CH_3)_2$, 6H), 1.11 (d, J_{Pt-H} = 65.6 Hz, J_{F-H} = 7 Hz, Pt−CH_3, 3H), 0.72 (d, J_{Pt-H} = 68.3 Hz, J_{F-H} = 7 Hz, Pt−CH_3, 3H). ^{19}F NMR (acetonitrile-d_3, 282 MHz): δ −101.8 (m, aryl F, 1F), −110.5 (m, aryl F, 1F), −260.9 (br s, Pt−F, 1F).

[PtMe$_2$Br(SMe$_2$)(C$_6$FCH═NCH$_2$C$_6$H$_5$)] ***(3)***. Based on in situ NMR spectroscopic characterization, 95% conversion based on integration of the ^{19}F NMR spectrum. ^1H NMR (acetonitrile-d_3, 300 MHz): δ 8.73 (s, J_{Pt-H} = 45.0 Hz, CH═N, 1H), 7.80−6.52 (m, overlapping peaks, aryl H), 4.84 (m, CH_2, 2H), 1.87 (s, J_{Pt-H} = 12.0 Hz, Pt−$S(CH_3)_2$, 6H), 1.07 (s, J_{Pt-H} = 68.4 Hz, Pt−CH_3, 3H), 0.71 (s, J_{Pt-H} = 69.6 Hz, Pt−CH_3, 3H). ^{19}F NMR (acetonitrile-d_3, 282 MHz): δ −114.6 (d, J = 10 Hz, aryl F, 1F).

[Pt(CD$_3$)$_2$F(SMe$_2$)(C$_6$F$_2$CH═NCH$_2$C$_6$H$_5$)] ***(13)***. In a 20 mL vial in the glovebox, *N*-(2,4,6-trifluorobenzylidene)benzylamine (0.080 g, 0.032 mmol, 1.0 equiv) and $Pt_2(CD_3)_4(SMe_2)_2$ (0.94 g, 0.016 mmol, 0.5 equiv) were dissolved in CD_3CN (1.0 mL). The resulting solution was transferred into an NMR tube, which was then fitted with a screw cap containing a septum. The reaction was monitored by ^1H and ^{19}F NMR spectroscopy: >95% conversion based on in situ NMR spectroscopic characterization. ^1H NMR (acetonitrile-d_3, 300 MHz): δ 8.78 (s, J_{Pt-H} = 47.1 Hz, CH═N, 1H), 7.80−6.60 (m, overlapping peaks, aryl H), 5.05 (m, CH_2, 2H), 1.89 (s, J_{Pt-H} = 12.0 Hz, $S(CH_3)_2$, 6H). As expected, there were no resonances for Pt−CD_3 signals. ^{19}F NMR (acetonitrile-d_3, 282 MHz): δ −102.0 (m, aryl F, 1F), −110.7 (m, aryl F, 1F), −261.8 (br s, Pt−F, 1F).

General Procedure for Preparation of Me_2Pt^{IV}−F·PPh_3 Complexes. In a 20 mL vial in the glovebox, the substrate (0.085 g, 0.034 mmol, 1.0 equiv) and $Pt_2Me_4(SMe_2)_2$ (0.098 g, 0.017 mmol, 0.5 equiv) were dissolved in CD_3CN (1.0 mL). The vial was left to stand for 24 h, after which triphenylphosphine (0.090 g, 0.034 mmol, 1.0 equiv) was added into the vial. The vial was stirred until complete dissolution of the triphenylphosphine; the sample was then transferred to a screw-cap NMR tube and removed from the glovebox. The reaction was monitored by ^1H, ^{19}F, and $^{31}P\{^1H\}$ NMR spectroscopy over 24 h.

[PtMe$_2$F(PPh$_3$)(C$_6$F$_4$CH═NCH$_2$C$_6$H$_4$Br)] ***(4)***. Colorless crystals were obtained from a saturated solution of acetonitrile; 40% yield. ^1H NMR (acetonitrile-d_3, 300 MHz): δ 8.56 (s, J_{Pt-H} = 36.9 Hz, CH═N, 1H), 7.76−7.23 (m, overlapping peaks, aryl H), 4.58 (m, CH_2, AB pattern, 2H), 1.62 (dd, J_{Pt-H} = 59.4 Hz, J_{F-H} = 12 Hz, J_{P-H} = 5 Hz, Pt−CH_3, 3H), 0.74 (dd, J_{Pt-H} = 61.0 Hz, J_{F-H} = 12 Hz, J_{P-H} = 5 Hz, Pt−CH_3, 3H). ^{19}F NMR (acetonitrile-d_3, 282 MHz): δ −126.1 (m, aryl F, 1F), −139.6 (m, aryl F, 1F), −148.1 (m, aryl F, 1F), −164.1 (m, aryl F, 1F), −273.5 (s, J_{Pt-H} = 31.0 Hz, Pt−F, 1F). $^{31}P\{^1H\}$ NMR (acetonitrile-d_3, 121 MHz): δ −0.57 (d, J_{Pt-H} = 1614 Hz, J_{P-F} = 52 Hz, Pt−PPh_3). HRMS (ESI positive ion mode): m/z calcd for $C_{34}H_{27}F_5NP^{79}Br^{194}Pt$: 848.0611, found 848.0608.

[PtMe$_2$F(PPh$_3$)(C$_6$F$_2$CH═NCH$_2$C$_6$H$_5$)] ***(5)***. Based on in situ NMR spectroscopic characterization, 70% conversion based on integration of the ^{19}F NMR spectrum. ^1H NMR (acetonitrile-d_3, 300 MHz): δ 8.23 (s, J_{Pt-H} = 55.2 Hz, CH═N, 1H), 7.66−6.28 (m, overlapping signals, aryl H), 4.95−4.30 (m, overlapping signals, CH_2, 2H), 1.22 (td, J_{Pt-H} = 66.0 Hz, J_{P-H} = 8 Hz, J_{F-H} = 2 Hz, Pt−CH_3, 3H), 0.62 (td, J_{Pt-H} = 61.8 Hz, J_{F-H} = 8 Hz, J_{P-H} = 2 Hz, Pt−CH_3, 3H). ^{19}F NMR (acetonitrile-d_3, 282 MHz): δ −101.8 (m, aryl F, 1F), −110.5 (m, aryl F, 1F), −281.3 (m, Pt−F, 1F). $^{31}P\{^1H\}$ NMR (acetonitrile-d_3, 121 MHz): δ −1.72 (d, J_{Pt-P} = 1102 Hz, J_{P-F} = 64 Hz, Pt-PPh_3). HRMS (ESI positive ion mode): m/z calcd for $C_{34}H_{31}F_3NP^{194}Pt$ 736.1794, found 736.1782.

[PtMe$_2$Br(PPh$_3$)(C$_6$FCH═NCH$_2$C$_6$H$_5$)] ***(6)***. Colorless crystals were obtained from a saturated solution of acetonitrile; 53% yield. ^1H NMR (dichloromethane-d_2, 300 MHz): δ 8.11 (s, J_{Pt-H} = 49.8 Hz, CH═N, 1H), 7.55−7.49 (t, J = 8.7 Hz, 1H), 7.40−7.28 (m, signals overlapping with PPh_3, aryl H), 7.04 (dd, J = 6.6 Hz, J = 4 Hz, 2H), 6.88 (d, AB pattern, J = 8 Hz), 6.65 (t, J = 9.0 Hz, 1H), 6.45 (d, J_{Pt-H} = 43.8 Hz, 1H), 5.03 (d, AB pattern, J = 18.3 Hz). 1.49 (d, Pt−CH_3, J_{H-P} = 8 Hz, J_{Pt-H} = 69.3 Hz, 3H), 0.98 (d, Pt−CH_3, J_{H-P} = 8 Hz, J_{Pt-H} = 58.2 Hz, 3H). ^{19}F NMR (dichloromethane-d_2, 282 MHz): δ −114.0 (m, J_{Pt-F} = 42 Hz, aryl F). $^{31}P\{^1H\}$ NMR (dichloromethane-d_2, 121 MHz): δ −7.2 (s, J_{Pt-P} = 1006 Hz, Pt−PPh_3). $^{13}C\{^1H\}$ NMR (dichloromethane-d_2, 150 MHz): 166.1 (s, J_{Pt-C} = 54.8 Hz), 161.1 (d, J_{F-C} = 965.0 Hz, J_{Pt-C} = 51.3 Hz), 151.5 (d, J_{F-C} = 21.4 Hz, J_{Pt-C} = 932.7 Hz), 136.3 (s), 134.4 (s), 131.3 (d, J_{P-C} = 33.8 Hz), 130.9 (d, J_{F-C} = 146.0 Hz, J_{Pt-C} = 11.4 Hz), 130.6 (s), 130.4 (d, J_{F-C} = 9.0 Hz), 130.2 (d, J_{F-C} = 29.9 Hz), 129.2 (s), 128.5 (s), 128.4 (d, J_{P-C} = 18.5 Hz), 124.6 (d, J_{F-C} = 16.9 Hz, J_{Pt-C} = 41.0 Hz), 60.5 (s, J_{Pt-C} = 12.6 Hz), 10.56 (s, J_{Pt-C} = 491.6 Hz), −4.43 (d, J_{P-C} = 7.0 Hz, J_{Pt-C} = 618.0 Hz). HRMS (ESI positive ion mode): m/z calcd for $C_{34}H_{32}{}^{79}BrFNP^{194}Pt$ 779.1084, found 779.1086. Anal. Calcd for $C_{34}H_{32}BrFNPPt$: C, 54.69; H, 4.20; N, 1.82. Found: C, 55.10; H, 4.34; N, 1.60.

[PtMe$_2$F(PPh$_3$)(C$_6$F$_4$CH═NCH$_2$C$_6$H$_5$)] ***(10)***. Based on in situ NMR spectroscopic characterization, 42% conversion based on integration of the ^{19}F NMR spectrum. ^1H NMR (acetonitrile-d_3, 300 MHz): δ 8.71 (s, J_{Pt-H} = 39.0 Hz, CH═N, 1H), 7.50 −7.31 (m, overlapping peaks, aryl H), 4.66 (dd, J_{H-H} = 10.8 Hz, CH_2, AB pattern, 2H), 1.72 (dd, J_{Pt-H} = 58.5 Hz, J_{F-H} = 12 Hz, J_{P-H} = 5 Hz, Pt−CH_3, 3H), 0.72 (dd, J_{Pt-H} = 62.0 Hz, J_{F-H} = 12 Hz, J_{P-H} = 5 Hz, Pt−CH_3, 3H). ^{19}F NMR (acetonitrile-d_3, 282 MHz): δ −124.9 (m, aryl F, 1F), −141.1 (m, aryl F, 1F), −150.3 (m, aryl F, 1F), −165.6 (m, aryl F, 1F), −275.6 (s, J_{Pt-H} = 32.0 Hz, Pt−F, 1F). $^{31}P\{^1H\}$ NMR (acetonitrile-d_3, 121 MHz): δ −2.0 (d, J_{Pt-H} = 999 Hz). HRMS (ESI positive ion mode): m/z calcd for $C_{34}H_{29}F5NP^{194}Pt$ 772.1606, found 772.1612.

General Procedure for Preparation of Me_3Pt^{IV}·SMe_2 Complexes. In a 20 mL vial in the glovebox, substrate (0.085 g, 0.034 mmol, 1.0 equiv) and $Pt_2Me_4(SMe_2)_2$ (0.098 g, 0.017 mmol, 0.5 equiv) were dissolved in CD_3CN (1.0 mL). Me_2Zn (20 μL, 0.040 mmol, 2.0 M solution in toluene) was subsequently added by syringe. The resulting solution was transferred to an NMR tube, which was then fitted with a screw cap containing a septum. The NMR tube was removed from the glovebox. The reaction was monitored by ^1H and ^{19}F NMR spectroscopy.

[PtMe$_3$(SMe$_2$)(C$_6$F$_2$CH═NCH$_2$C$_6$H$_5$)] ***(8)***. Based on in situ NMR spectroscopic characterization, >95% conversion from Pt^{IV}−F·SMe_2 complex **2** based on integration of the ^1H NMR spectrum. ^1H NMR (acetonitrile-d_3, 300 MHz): δ 8.86 (s, J_{Pt-H} = 40.0 Hz, 1H, CH═N), 7.37−7.13 (m, overlapping peaks, aryl H), 4.99 (m, CH_2, 2H), 1.78 (s, J_{Pt-H}= 13.0 Hz, $S(CH_3)_2$, 6H), 0.75 (s, J_{Pt-H} = 69.0 Hz, Pt−CH_3, 3H),

0.36 (s, J_{Pt-H} = 73.1 Hz, Pt−CH_3, 3H), 0.16 (s, J_{Pt-H} = 46.0 Hz, Pt−CH_3, 3H). ^{19}F NMR (acetonitrile-d_3, 282 MHz): δ −104.3 (m), −111.6 (m).

*[PtMe$_3$(SMe$_2$)(C$_6$F$_4$CH═NCH$_2$C$_6$H$_5$)] (**14**).* Based on in situ NMR spectroscopic characterization, >95% conversion from the corresponding Pt^{IV}−F·SMe$_2$ complex based on integration of the ^{1}H NMR spectrum. ^{1}H NMR (acetonitrile-d_3, 300 MHz): δ 8.90 (s, J_{Pt-H} = 39.0 Hz, 1H, CH═N), 7.55−6.87 (m, overlapping signals, aryl H), 4.96 (br m, CH_2, 2H), 1.89 (s, J_{Pt-H} = 12.6 Hz, 6H, Pt−S(CH_3)$_2$), 1.09 (d, J_{F-H} = 3 Hz, J_{Pt-H} = 70.8 Hz, 3H, Pt−CH_3), 0.53 (s, J_{Pt-H} = 72.0 Hz, 3H, Pt−CH_3), 0.35 (s, J_{Pt-H} = 33.0 Hz, 3H, Pt−CH_3). ^{19}F NMR (acetonitrile-d_3, 282 MHz): δ −129.0 (dd, J = 28 Hz, J = 21 Hz, 1F), −147.9 (m, 1F), −151.8 (dd, J = 28 Hz, J = 18 Hz, 1F), −155.2 (m, 1F).

*[PtMe$_3$(SMe$_2$)(C$_6$F$_2$CH═NCH$_2$C$_6$H$_5$)] (**15**).* Based on in situ NMR spectroscopic characterization, >95% conversion from the corresponding Pt^{IV}−F·SMe$_2$ complex based on integration of the ^{1}H NMR spectrum. ^{1}H NMR (acetonitrile-d_3, 300 MHz): δ 8.97 (s, J_{Pt-H} = 38.4 Hz, 1H, CH═N), 7.36−7.13 (m, overlapping peaks, aryl H), 6.96−6.89 (m, 1H), 6.74 (td, J = 9.0 Hz, J = 3.6 Hz, 1H), 4.97 (br m, 2H, CH_2), 1.88 (s, J_{Pt-H} = 13.2 Hz, 6H, Pt−S(CH_3)$_2$), 1.08 (d, J_{F-H} = 3 Hz, J_{Pt-H} = 71.4 Hz, 3H, Pt−CH_3), 0.53 (s, J_{Pt-H} = 73.2 Hz, 3H, Pt−CH_3), 0.28 (s, J_{Pt-H} = 48.6 Hz, 3H, Pt−CH_3). ^{19}F NMR (acetonitrile-d_3, 282 MHz): δ −105.4 (d, J_{F-H} = 25 Hz, J_{Pt-F} = 302 Hz, 1F), −121.1 (dm, J_{Pt-F} = 261 Hz, 1F).

[Pt(CD$_3$)$_2$Me(SMe$_2$)(C$_6$F$_2$CH═NCH$_2$C$_6$H$_5$)]: Deuterium Labeling Study. To a solution of complex **13** was added Me$_2$Zn (20 μL, 0.042 mmol, 2.0 M solution in toluene) by syringe. The reaction was monitored by ^{1}H and ^{19}F NMR spectroscopy. Three resonances for the three methyl groups appeared with a ratio of 1:1:1; >95% conversion from Pt^{IV}−F·SMe$_2$ complex **13** based on integration of the ^{1}H NMR spectrum. ^{1}H NMR (acetonitrile-d_3, 300 MHz): δ 8.86 (s, J_{Pt-H} = 39.2 Hz, CH═N, 1H), 7.70−6.60 (m, overlapping peaks, aryl H), 4.98 (m, CH_2, 2H), 1.78 (s, J_{Pt-H} = 13.2 Hz, S(CH_3)$_2$, 6H), 0.74 (s, J_{Pt-H} = 69.6 Hz, Pt−CH_3, 3H) (overlapped three singlets), 0.36 (s, J_{Pt-H} = 72.8 Hz, Pt−CH_3, 3H) (overlapped three singlets), 0.15 (s, J_{Pt-H} = 44.8 Hz, Pt−CH_3, 3H) (overlapped three singlets).

General Procedure for Preparation of Me$_3$Pt^{IV}·PPh$_3$ Complexes. In the glovebox, a solution of the Me$_3$Pt^{IV}·SMe$_2$ complex was combined with triphenylphosphine (0.090 g, 0.034 mmol, 1.0 equiv). The vial was stirred until complete dissolution of the triphenylphosphine, after which the sample was transferred to a screw-cap NMR tube and removed from the glovebox. The reaction was monitored by ^{1}H, ^{19}F, and ^{31}P{^{1}H}NMR spectroscopy over 24 h. The complexes could also be prepared by initial formation of the corresponding Pt^{IV}−F·PPh$_3$ complex followed by transmetalation with Me$_2$Zn. Accordingly, inside the glovebox a solution of Me$_2$Pt^{IV}−F·PPh$_3$ was combined with Me$_2$Zn (20 μL, 0.040 mmol, 2.0 M solution in toluene), which was added via microsyringe. The resulting solution was transferred to a screw-cap NMR tube, sealed, and removed from the glovebox. Reaction progress was monitored by ^{1}H, ^{19}F, and ^{31}P{^{1}H} NMR spectroscopy.

*[PtMe$_3$(PPh$_3$)(C$_6$F$_5$CH═NCH$_2$C$_6$H$_5$)] (**11**).* Pink crystals were obtained by layering pentanes on a saturated solution of dichloromethane; 46% yield. ^{1}H NMR (acetonitrile-d_3, 300 MHz); δ 8.48 (s, J_{Pt-H} = 41.1 Hz, CH═N, 1H), 7.45−7.07 (m, overlapping peaks, aryl H), 4.39 (dd, J_{H-H} = 15.6 Hz, CH_2, 2H, AB pattern), 1.38 (dd, J_{Pt-H} =70.5 Hz, J_{Pt-P} = 8 Hz, J_{F-H} = 2 Hz, Pt−CH_3, 3H), 0.66 (dd, J_{Pt-H} = 48.0 Hz, J_{Pt-P} = 8 Hz, Pt−CH_3, 3H), 0.46 (dd, J_{Pt-H} = 63.8 Hz, J_{P-H} = 8 Hz, Pt−CH_3, 3H). ^{19}F NMR (acetonitrile-d_3, 282 MHz): δ − 126.6 (m, aryl F, 1F), −142.9 (m, aryl F, 1F), −152.2 (m, aryl F, 1F), −167.4 (m, aryl F, 1F). ^{31}P{^{1}H} NMR (acetonitrile-d_3, 121 MHz): δ −7.08 (s, J_{Pt-P} = 1038 Hz). ^{13}C{^{1}H} NMR (dichloromethane-d_2, 100 MHz): δ 169.2 (br s), 154.7 (s), 151.8 (dm, J_{F-C} = 230 Hz), 148.8 (dm, J_{F-C} = 262 Hz), 143.5 (dm, J_{F-C} = 266 Hz), 137.2 (m, overlaps with resonances for PPh$_3$), 134.5 (t, J_{Pt-C} = 7.6 Hz, overlaps with resonances for PPh$_3$), 134.3 (d, J_{P-C} = 10 Hz), 132.6 (s), 132.1 (s), 131.8 (d, J_{Pt-C} = 10.8 Hz, J_{P-C} = 38 Hz), 130.7 (d, J_{P-C} = 2 Hz), 128.6 (d, J_{P-C} = 8 Hz), 122.9 (s), 59.2 (s, J_{Pt-C} = 14.5 Hz), 7.29 (d, J_{Pt-C} = 543.4 Hz, J_{P-C} = 115 Hz), 2.17 (br, s. J_{Pt-C} = 478.0 Hz), −12.9 (dd, J_{Pt-C} = 613.9 Hz, J_{P-C} = 11 Hz, J_{F-C} = 4 Hz). HRMS (ESI positive ion mode): calcd for $C_{35}H_{32}F_4NP^{194}Pt$ 768.1856, found 768.1860. Anal. Calcd for $C_{35}H_{32}F_4NPPt$: C, 54.69; H, 4.20; N, 1.82. Found: C, 54.73; H, 4.45; N, 1.95.

■ ASSOCIATED CONTENT

Supporting Information

Text, figures, tables, and CIF files giving complete experimental details and characterization data for all compounds and crystallographic data for the solid-state molecular structures. This material is available free of charge via the Internet at http://pubs.acs.org.

■ ACKNOWLEDGMENTS

We thank the following for support of this research: NSERC (Discovery, Research Tools and Instrumentation Grants) and the University of British Columbia.

■ REFERENCES

(1) For recent reviews on the use of transition metals in organic synthesis, see: (a) Wang, C.; Xi, Z. *Chem. Soc. Rev.* **2007**, *36*, 1395−1406. (b) Forke, R.; Gruner, K. K.; Knott, K. E.; Auschill, S.; Agarwal, S.; Martin, R.; Bohl, M.; Richter, S.; Tsiavaliaris, G.; Fedorov, R.; Manstein, D. J.; Gutzeit, O.; Knolker, H.-J. *Pure Appl. Chem.* **2010**, *82*, 1975−1991. (c) Gluech, D. S. *Dalton Trans.* **2008**, *39*, 5276−5286. (d) Majumdar, K. C.; Debnath, P. D. N.; Roy, B. *Curr. Org. Chem.* **2011**, *15*, 1760−1801. (e) Luh, T.-Y.; Leung, M.-K.; Wong, K.-T. *Chem. Rev.* **2000**, *100*, 3187−3204.

(2) Cotton, F. A.; Wilkinson, G.; Murillo, C. A.; Bochmann, M. *Advanced Inorganic Chemistry*, 6th ed.; Wiley: New York, 1999.

(3) For recent reviews of stoichiometric C−F activation, see: (a) Amii, H.; Uneyma, K. *Chem. Rev.* **2009**, *109*, 2119−2183. (b) Perutz, R. N.; Braun, T. Transition Metal-Mediated C-F Bond Activation. In *Comprehensive Organometallic Chemistry*; Mingos, D. M. P., Crabtree, R. H., Eds.; Elsevier: Amsterdam, 2007.

(4) Sun, A. D.; Love, J. A. *Dalton Trans.* **2010**, *39*, 10362−10374.

(5) (a) Muller, K.; Faeh, C.; Diedrich, F. *Science* **2007**, *317*, 1881−1886. (b) Bohm, H.-J.; Banner, D.; Bendels, S.; Kansy, M.; Kuhn, B.; Muller, K.; Obst-Sanch, U.; Stahl, M. *ChemBioChem* **2004**, *5*, 637−643.

(6) For recent examples see: (a) Hong, S.; Lee, J.; Kim, M.; Park, Y.; Park, C.; Kim, M.-H.; Jew, S.-S.; Park, H. *J. Am. Chem. Soc.* **2011**, *133*, 4924−4929. (b) Welsh, G. C.; Bazan, G. C. *J. Am. Chem. Soc.* **2011**, *133*, 4632−4644. (c) Price, S. C.; Stuart, A. C.; Yang, L.; Zhou, H.; You, W. *J. Am. Chem. Soc.* **2011**, *133*, 4625−4631. (d) Nguyen, J. D.; Tucker, J. W.; Konieczynska, M. D.; Stephenson, R. J. *J. Am. Chem. Soc.* **2011**, *133*, 4160−4163. (e) Zhao, Q.; Yu, M.; Shi, L.; Liu, S.; Li, C.; Shi, M.; Zhou, Z.; Huang, C.; Li, F. *Organometallics* **2010**, *29*, 1085−1091. (f) Schelter, E. J.; Yang, P.; Scott, B. L.; Thompson, J. D.; Martin, R. L.; Hay, J. P.; Morris, D. E.; Kiplinger, J. C. *Inorg. Chem.* **2007**, *46*, 7477−7488. (g) Hughes, R.; Smith, J. M.; Incarvito, C. D.; Lam, K.-C.; Rhatigan, B.; Rheingold, A. C. *Organometallics* **2002**, *21*, 2136−2144.

(7) For selected examples see: (a) Noveski, D.; Braun, T.; Schulte, M.; Neumann, B.; Stammler, H. *Dalton Trans.* **2003**, 4075−4083. (b) Jones, W. D.; Partridge, M. G.; Perutz, R. N. *Chem. Commun.* **1991**, 264−266. (c) Edelbach, B. L.; Jones, W. D. *J. Am. Chem. Soc.* **1997**, *119*, 7734−7742. (d) Blum, O.; Frolow, F.; Milstein, D. L. *Chem. Commun.* **1991**, 258−259. (e) Hughes, R. P.; Lartichev, R. B.; Zakharov, L. N.; Rheingold, A. L. *J. Am. Chem. Soc.* **2004**, *126*, 2308−2309.

(8) For selected examples see: (a) Braun, T.; Perutz, R. N. *Chem. Commun.* **2002**, 2749−2757. (b) Schaub, T.; Fischer, P.; Steffen, A.; Braun, T.; Radius, U.; Mix, A. *J. Am. Chem. Soc.* **2008**, *130*, 9304−9317. (c) Fahey, D. R.; Mahan, J. E. *J. Am. Chem. Soc.* **1977**, *99*, 1101−1108. (d) Johnson, S. A.; Huff, C. W.; Mustafa, F.; Saliba, M. *J. Am. Chem. Soc.* **2008**, *130*, 17279−17280.

(9) For selected examples see: (a) Bruce, M. I.; Goodall, B. C.; Sheppard, G. L.; Stone, F. G. A. *Dalton Trans.* **1975**, 591−595. (b) Klahn, A. H.; Moore, M. H.; Perutz, R. N. *Chem. Commun.* **1992**, 1699−1701. (c) Mohr, W.; Stark, G. A.; Jiao, H.; Gladysz, J. A. *Eur. J. Inorg. Chem.* **2001**, *4*, 925−933. (d) Dietz, T. G.; Chatellier, D. S.; Ridge, D. P. *J. Am. Chem. Soc.* **1978**, *100*, 4905−4907. (e) Bjornson, A.; Taylor, J. W. *Organometallics* **1989**, *8*, 2020−2024. (f) Chernega, A. N.; Grahan, A. J.; Green, M. L. H.; Haggitt, J.; Lloyd, J.; Mehnert, C. P.; Metzler, N.; Souter, J. *Dalton Trans.* **1997**, 2293−2303. (g) Barrio, P.; Castarlenos, R.; Esteruelas, M. A.; Lledos, A.; Maseras, F.; Onate, E.; Tonas, J. *Organometallics* **2001**, *20*, 442−452. (h) Arrayo, M.; Bernes, S.; Ceron, M.; Cartina, V.; Mendoza, C.; Torrens, H. *Inorg. Chem.* **2007**, *46*, 4857−4867.

(10) (a) Kiso, Y.; Tamao, K.; Kumada, M. *J. Organomet. Chem.* **1973**, *50*, C12−C14. (b) Cahoez, G.; Lepifre, F.; Ramiandrasoa, P. *Synthesis* **1999**, 2138−2140. (c) Edelbach, B. L.; Kraft, B. M.; Jones, W. D. *J. Am. Chem. Soc.* **1999**, *121*, 10327−10331. (d) Bohm, V. P. W.; Gstoltmayr, L. W. K.; Weskamp, T.; Hermann, W. A. *Angew. Chem., Int. Ed.* **2001**, *113*, 3500−3502. (e) Ackermann, L.; Born, R.; Spatz, J. H.; Meyer, D. *Angew. Chem., Int. Ed.* **2005**, *117*, 7382−7340. (f) Widdowson, D. A.; Wilhelm, R. *Chem. Commun.* **1999**, 2211−2212. (g) Mikami, K.; Miyamoto, T.; Hatano, M. *Chem. Commun.* **2004**, 2082−2083. (h) Kim, Y. M.; Yu, S. *J. Am. Chem. Soc.* **2003**, *125*, 1696−1697. (i) Bahmanyar, S.; Borer, B. C.; Kim, Y. M.; Kurtz, D. M.; Yu, S. *Org. Lett.* **2005**, *8*, 1101−1014. (j) Braun, T.; Perutz, R. N.; Sladek, M. I. *Chem. Commun.* **2001**, 2254−2255. (k) Yoshikai, N.; Mashima, H.; Nakamura, E. *J. Am. Chem. Soc.* **2005**, *127*, 17978−17979. (l) Schaub, T.; Backes, M.; Radius, U. *J. Am. Chem. Soc.* **2006**, *128*, 15964−15965. (m) Sacki, T.; Takashima, Y.; Tamao, K. *Synlett.* **2005**, *7*, 1771−1774. (n) Manabe, K.; Ishikawa, S. *Synthesis* **2008**, 2645−2649. (o) Arisawa, M.; Suzuki, T.; Ishikawa, T.; Yamaguchi, M. *J. Am. Chem. Soc.* **2008**, *130*, 12214−12215.

(11) (a) Wang, T.; Alfonso, B. J.; Love, J. A. *Org. Lett.* **2007**, *9*, 5629−5631. (b) Sun, A. D.; Love, J. A. *J. Fluorine Chem.* **2010**, *131*, 1237−1240.

(12) For relatedexamplesof methoxylation, see: Buckley, H.; Wang, T.; Tran, O.; Love, J. A. *Organometallics* **2009**, *28*, 2356−2359.

(13) For detailed informationregarding the identification and characterization of a Me_3Pt^{IV} complex, see: Wang, T.; Love, J. A. *Organometallics* **2008**, *27*, 3290−3296.

(14) For selected examples of Pt-catalyzed C−X bond activation, see: (a) Rashidi, M.; Esmaeilbeig, A. R.; Shakabadi, N.; Tangestaninejad, S.; Puddephatt, R. J. *J. Organomet. Chem.* **1998**, *568*, 53−61. (b) Song, D.; Sliwowski, K.; Pang, J.; Wang, S. *Organometallics* **2002**, *21*, 4978−4985. For a review of Pt-catalyzed C−Hactivation, see: Shilov, A. E.; Shul'pin, G. B. *Chem. Rev.* **1997**, *97*, 2879−2932.

(15) Complex **2** has been previously reported.[16a]

(16) (a) Crespo, M.; Martinez, M.; Sales, J. *Organometallics* **1994**, *13*, 706−720. (b) Crespo, M.; Martinez, M.; de Pablo, E. *Dalton Trans.* **1997**, 1231−1235. (c) Crespo, M.; Granell, J.; Solans, X.; Font-Bardia., M. *Organometallics* **2002**, *21*, 5140−5143. (d) Calvet, T.; Crespo, M.; Font-Bardia, M; Gomez, K.; Gonzalez, G.; Martinez, M. *Organometallics* **2009**, *28*, 5096−5106. (e) Bernhardt, P. V.; Gallego, C.; Martinez, M. *Organometallics* **2000**, *19*, 4862−4869.

(17) For all Pt(IV) complexes, the signal in the ^{1}H NMR spectrum corresponding to the Pt−SMe_2 ligand was observed as a singlet from δ 1.96 to 1.87 (J_{Pt-H} = 12.0 Hz). The lack of diastereotopic methyl signals is postulated to be the result of rapid inversion about the Pt−S bond at room temperature. A variety of metal−thioether complexes have been reported in which the sulfur ligand was found to undergo rapid inversion at room temperature, forming diastereotopic signals only upon cooling below −20 °C. For examples, see: (a) Mendez, N. Q.; Arif, A. M.; Gladysz, J. A. *Organometallics* **1991**, *10*, 2199−2209. (b) Abel, E. W.; Booth, M.; Orrell, K. G. *Dalton Trans.* **1980**, *9*, 1582−1592. (c) Abel, E. W.; Orrell, K. G.; Rahoo, H.; Sik, V. *J. Organomet. Chem.* **1992**, *437*, 191−199.

(18) See the Supporting Information for details.

(19) (a) van Asselt, R.; Rjinberg, E.; Elseiver, C. J. *Organometallics* **1994**, *13*, 706−720. (b) Clegg, D. E.; Hall, J. R.; Swile, G. A. *J. Organomet. Chem.* **1972**, *38*, 403−420. (c) Ruddick, J. R.; Shaw, B. L. *J. Chem. Soc. A* **1969**, 2969−2970.

(20) (a) Clark, H. C.; Manzer, L. E. *Inorg. Chem.* **1973**, *12*, 362−368. (b) Goldberg, K. I.; Yan, J.; Winter, E. L. *J. Am. Chem. Soc.* **1994**, *116*, 1573−1574. (c) Golberg, K. I.; Yan, J.; Breitung, E. M. *J. Am. Chem. Soc.* **1995**, *117*, 6889−6890.

(21) We switched to using the perfluoroarene, as the PPh_3 complex derived from **8** was too reactive. The increased stability of highly fluorinated Pt(IV) complexes likely results from formation of a stronger Pt−C_{aryl} bond. For examples of the effect of ligand electronics on M−C bond strength, see: (a) Hartwig, J. F. *Inorg. Chem.* **2007**, *46*, 1936−1947. (b) Holland, P. L.; Andersen, R. A.; Bergman, R. G.; Huang, J. K.; Nolan, S. P. *J. Am. Chem. Soc.* **1997**, *119*, 12800−12814. (c) Bryndza, H. E.; Fong, L. K.; Paciella, R. A.; Tam, W.; Bercaw, J. E. *J. Am. Chem. Soc.* **1987**, *109*, 1444−1456. (d) Clot, E.; Megret, C.; Eisenstein, O.; Perutz, R. N. *J. Am. Chem. Soc.* **2009**, *131*, 7817−7827. (e) Nova, A.; Erhardt, S.; Jasim, N. A.; Perutz, R. N. *J. Am. Chem. Soc.* **2008**, *130*, 15499−15511. (f) Tanabe, T.; Brennessel, W. W.; Clot, E.; Eisenstein, O.; Jones, W. D. *Dalton Trans.* **2010**, *39*, 10495−10509. (g) Evans, M. E.; Bruke, C. L.; Yaibuathes, S.; Clot, E.; Eisenstein, O.; Jones, W. D. *J. Am. Chem. Soc.* **2009**, *131*, 13464−13473.

(22) (a) Brown, M. P.; Puddephatt, R. J.; Upton, C. E. E. *Dalton Trans.* **1974**, 2457−2465. (b) Hill, G. S.; Puddephatt, R. J. *Organometallics* **1997**, *16*, 4522−4524. (c) Lanci, M. P; Remy, M. S.; Lao, D. B.; Sanford, M. S; Mayer, J. M. *Organometallics* **2011**, *30*, 3704−3707.

(23) No ethane formation was detected when experiments were performed in sealed J. Young tubes.

(24) Hill, G. S.; Irwin, M. J.; Levy, C. J.; Rendina, L. M.; Puddephatt, R. J.; Andersen, R. A.; McLean, L. *Inorg. Synth.* **1972**, *13*, 121−124.

(25) Krasovkiv, A.; Knochel, P. *Synthesis* **2006**, 890−891.